Continuous succinic acid fermentation by *Escherichia coli* KJ122 with cell recycle

Adolf Krige and Willie Nicol[a]

Department of Chemical Engineering, University of Pretoria, Lynnwood Road, Hatfield, 0002 Pretoria, South Africa

[a]Corresponding author: Tel.: +27124203796; Fax: +27124205048.E-mail: willie.nicol@gmail.com

***Graphical Abstract**

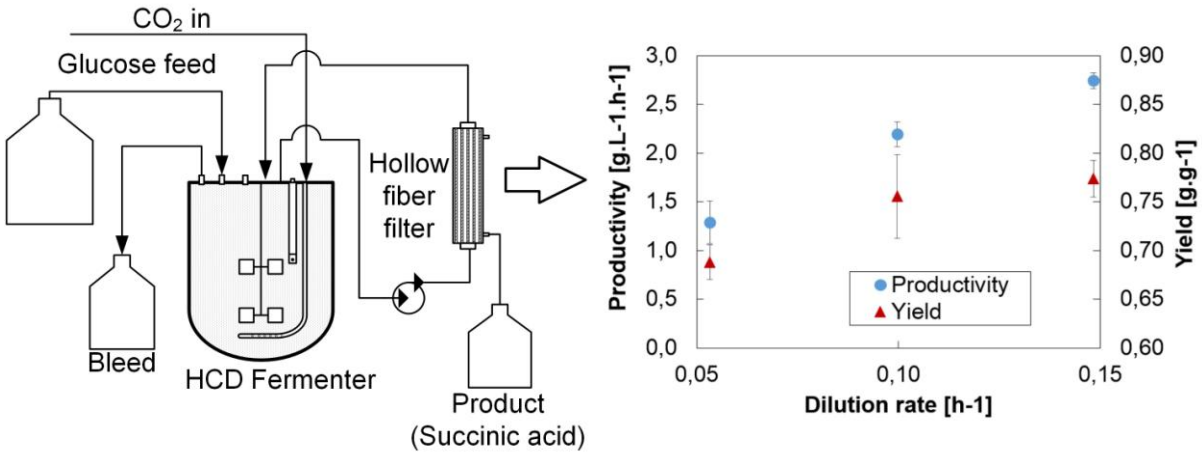

Highlights

- A productivity of 3 $g.L^{-1}.h^{-1}$and a yield of 0.77 $g.g^{-1}$were achieved at D = 0.15 h^{-1}
- Increased pyruvate dehydrogenase activity at higher D leads to increase in yield
- Minimal oxidative tricarboxylic acid (TCA)/glyoxylate flux was detected from analysis
- The batch results are inferior in productivity but superior in yield and titre

Abstract

High cell densities were obtained by separating the cells with an external hollow fibre filter. Extreme product inhibition at high succinate titres resulted in cell death and subsequent lysis. Accordingly, the highest succinate titre obtained during continuous fermentation was 25 $g.L^{-1}$ at a dilution rate of 0.05 h^{-1}. The highest volumetric productivity of 3 $g.L^{-1}.h^{-1}$ and the highest succinate yield (0.77 $g.g^{-1}$) were obtained at the highest dilution rate (0.15 h^{-1}). The improved yield was caused by increased pyruvate dehydrogenase activity, leading to a decrease in pyruvate and formate excretion and an increase in the reductive flux towards succinate as additional reduction power was produced. The oxidative tricarboxylic acid cycle flux was determined to be minimal, with most of the acetyl coenzyme A (acetyl-CoA) culminating as acetate. Although comparative batch fermentations exhibited a fivefold lower volumetric productivity than the maximum obtained in the cell recycle runs, higher succinate titres (56 $g.L^{-1}$) and yields (0.85 $g.L^{-1}$) were obtained. The higher batch yields were attributed to pyruvate and formate consumption after the termination of cell growth.

Keywords: Succinic acid, *Escherichia coli*, Continuous cell recycle, High-cell-density fermentation, Metabolic flux analysis

1 Introduction

In future biorefineries, sugar-derived fermentation products will replace numerous fossil-based chemical intermediates. The organic acid platforms form an integral part of these biobased replacement molecules, especially dicarboxylic acids, which allow various polymerization options. As expected, succinate is still considered one of the top 10 biobased products from biorefinery carbohydrates on the list of top biobased chemicals revisited by the U.S. Department of Energy.[1] Succinate can potentially replace a significant fraction of the petrochemical-derived maleic anhydride and 1,4-butanediol market from which the intermediate tetrahydrofuran is produced.[2]Tetrahydrofuran is the building block used to produce elastic fibres and engineer thermoplastics. Succinate is also likely to replace adipic acid in the production of polyurethane from polyester polyols.[3] In addition, the market for polybutylene succinate, a polyester consisting of succinate and its hydrogenated alcohol product (1,4-butanediol), is anticipated to grow rapidly within the next decade.[4]

Succinate is a natural fermentation product in the anaerobic metabolic pathway of several bacteria. Wild bacteria such as *Actinobacillussuccinogenes, Mannheimiasucciniciproducens and Anaerobiospirillumsucciniciproducens* have been extensively studied; although excellent final titre, productivity and yield have been obtained successfully, unwanted by-products such as acetate and formate remain a challenge.[3] In addition, the presence of complex nutrients in the growth medium poses a severe cost disadvantage.[5] From a metabolic engineering viewpoint, *Escherichia coli* is an ideal host as succinate is produced as part of the anaerobic catabolism of the wild strain. Accordingly, numerous groups have modified this host[6–10] in an attempt to achieve homosuccinate fermentation. The stoichiometric limitation of homosuccinate fermentation is well established, and it is theoretically possible to obtain a yield of 1.12 g of succinate per gram of glucose consumed.[11] To achieve this yield, the

oxidative part of the tricarboxylic acid (TCA) cycle or the glyoxylate shunt is used to generate the reduction power consumed in the reverse TCA pathway up to succinate.[11]

Jantama et al.[12] developed a succinate-producing *E. coli* strain KJ 122, which can grow in the absence of complex nitrogen sources. All the genes responsible for by-product formation were deleted, while the full TCA and glyoxylate cycle provided the oxidative machinery to prohibit, at least in theory, the necessary formation of by-products. The reported batch yields of 0.96 $g.g^{-1}$ suggest that either the oxidative TCA or glyoxylate cycle is used to generate reduction power, as redox balancing via acetate formation has a maximum theoretical yield of 0.87 $g.g^{-1}$ when biomass formation is ignored.[13]*E. coli* KJ122 still produced small amounts of acetate; although the acetate amount was slightly reduced by the inactivation of phosphotransacetylase (*E. coli* KJ134), acetate formation was not terminated. Despite these small amounts of acetate, the yield characteristics and nutrient requirements of *E. coli* KJ122 remain promising and warrant further studies on the organism under different fermentation conditions.

Historically, genetic engineering has placed emphasis on high-value, low-volume products, such as pharmaceutical proteins, which require significant downstream purification due to regulatory standards. In a biorefinery, the emphasis will be on low-value, high-volume products such as ethanol, succinate and lactate. Therefore, the productivity, yield and outlet titre of the fermenter will play a crucial role in ensuring the feasibility of the biorefinery.[2,14] Unfortunately, high titres typically lead to lower cell productivity, thereby decreasing the volumetric productivity. This effect can be countered by increasing the cell concentration, thus allowing higher throughputs and volumetric productivity at acceptable product titres. High-cell-density fermentation

(HCDF) is best suited for continuous operation in which a high cellular content is maintained in the fermenter by constant cell separation. With higher cell densities, the dilution rate is not limited by the maximum growth rate, and accordingly cell washout is not a concern.[15]

For suspended cell systems, such as *E. coli* fermentation, cell separation via tangential filtration and subsequent recycle is a preferred method of concentrating cells. Significant productivity increases have been reported without any negative effect on the yield. Using continuous cell recycle fermentation with *Lactobacillus paracasei* to produce lactate, Xuet al.[16]obtained a maximum volumetric productivity of 31.5 $g.L^{-1}.h^{-1}$, 10 times higher than that of fed-batch fermentations. During continuous cell recycle fermentation with *Debaryomyceshansenii*to produce xylitol, Cruz et al.[17] obtained volumetric productivities 4.2 times higher than those achieved during continuous fermentation without cell recycle. A repeated recycle system that cultured recombinant *E. coli*HB101(pPAKS2) producing penicillin acylase in a membrane cell recycle fermenter obtained >10 times higher productivities than a batch system with dry cell weight (DCW) concentrations of up to 145 $g.L^{-1}$.[18]

In the current study, the *E. coli* KJ122 strain of interest was tested under continuous high-cell-density conditions. The aim was to establish the titre–volumetric productivity boundary while monitoring variations in the catabolic flux distributions affecting the overall succinate yield. Batch runs were performed in parallel to evaluate the advantages/disadvantages of the high-cell-density process. In the open literature, the reported fermentations of *E. coli* KJ122 and its sister strain *E. coli* KJ134 are restricted to batch and chemostat fermentations.[11,12] However, this study presents the first continuous cell recycle fermentation of the strain. Succinate was produced using D-

glucose as the main substrate in a minimal medium. Cell separation was achieved by external recycle using a hollow fibre filter (HFF) to extract the product.

2 Materials and methods

2.1 Microorganism and inocula

The modified strain of *E. coli* (KJ 122) was acquired from the Department of Microbiology and Cell Science of the University of Florida, USA, and used for all fermentations. The details of the performed gene modifications are provided in Table 1. The culture stock was stored in a 66% $w.w^{-1}$ glycerol solution at −40 °C. The inocula were incubated at 37 °C and 100 $r.min^{-1}$ for 16–24 h in 50-mL Schott screw-capped bottles containing 30 mL of sterilized Luria-Bertani broth. Each inoculum was prepared from frozen stock cultures to prevent mutation. The purity of the inocula was tested by high-performance liquid chromatography (HPLC).The strain did not produce lactate or ethanol in detectable quantities and the inoculum was therefore deemed infected if either was detected.

2.2 Medium

Unless specified otherwise, all chemicals used in the fermentations were obtained from Merck KgaA (Darmstadt, Germany). A defined medium (AM1), developed by Martinez et al.,[19] was used in all the fermentations. The concentrations specified for AM1 was used for all fermentations, except for one batch run, where all concentrations apart from glucose were increased by 50%. The medium was supplemented with 50 $g.L^{-1}$ D-glucose for continuous fermentations and 90–100 $g.L^{-1}$ D-glucose for batch fermentations, as the carbon source. CO_2 gas (Afrox, Johannesburg, South Africa)

Table 1: The relevant gene modifications made to *E. coli* C to obtain succinate-producing *E. coli* KJ 122[11,12]

Enzyme	Modification	Abbreviation
2-Ketobutyrate formate lyase	Inactivation	Δ tdcE
Acetate kinase	Inactivation	Δ ackA
Alcohol dehydrogenase	Inactivation	Δ adhE
Aspartate aminotransferase	Inactivation	Δ aspC
Citrate lyase	Inactivation	Δ citF
Formate transporter	Inactivation	Δ focA
Lactate dehydrogenase	Inactivation	Δ ldhA
Methylglyoxal synthase	Inactivation	Δ mgsA
NAD+-linked malic enzyme	Inactivation	Δ sfcA
PEP carboxykinase	Overexpression	pck+
Pyruvate formate lyase	Inactivation	Δ pflB
Pyruvate oxidase	Inactivation	Δ poxB
Threonine decarboxylase	Inactivation	Δ tdcD

was fed into the reactor as an inorganic carbon source at 0.1 vvm. Antifoam Y30 (0.5–1 $g.L^{-1}$; Sigma–Aldrich, St. Louis, MO, USA) was also added to prevent foaming.

2.3 Analytical methods

An Agilent 1260 Infinity HPLC device (Agilent Technologies,Santa Clara, CA, USA) was used to determine the concentrations of glucose, ethanol and organic acids. The HPLC device was equipped with a refractive index detector and a 300 × 7.8-mm Aminex HPX-87H column (Bio-Rad Laboratories,Hercules, CA, USA). A H_2SO_4 solution (0.3 $ml.L^{-1}$) was used as the mobile phase, at a column temperature of 60 °C. A 20-mL sample was taken from the bioreactor and centrifuged for 90 s at 17,000 $r.min^{-1}$. The supernatant fluid was filtered with a 0.2-µm filter, and 500 µL of the filtered sample was then transferred to an HPLC sampling vial and diluted with 1000 µL of filtered, distilled water.

For determining the cell density, the optical density (OD) at 660 nm and the DCW were measured. On comparing the OD measurements with the DCW, the continuous fermentation results showed a strong linear correlation between the data points, with an R^2 value of 0.88. However, the batch fermentations showed a weaker linear correlation, with an R^2 value of only 0.5. Therefore, only the DCW was used because it was considered to represent cell density better, especially as batch and continuous fermentations are compared in this study.

To calculate the DCW, the supernatant was drained after centrifugation, and the cell pellet was washed twice with distilled water, centrifuged between washes, and resuspended in distilled water. The sample was dried in an oven for at least 24 h at 85 °C before being weighed. Small values of biomass concentration (DCW < 0.4 $g.L^{-1}$) were considered inaccurate due to unavoidable errors in weighing the vials.

2.4 Batch fermentations

A 1.5-L Jupiter 2.0 (Solaris Biotechnology, Mantua, Italy) autoclavable fermentation system was used for all fermentations (Fig. 1). The temperature was controlled at 37 °C, while the pH was maintained at 7 by a separate controller (Liquiline, Endress+Hauser) and a pH probe (ISFET Sensor CPS471D, Endress+Hauser) to monitor the KOH dosing flow rate. An external Brooks mass flow controller was used to control the CO_2 inlet flow rates. The mass flow controller, pH controller and pumps were linked to customized LabVIEW (National Instruments) software via a National Instruments cDAQ-9184 module. All gas inlets and outlets contained 0.2-µm polytetrafluoroethylenemembrane filters (Midisart 2000, Satorius, Göttingen, Germany).

For both the continuous and batch fermentations, the reactor, tubes, medium reservoirs and the HFF (for continuous cell recycle fermentations) were autoclaved together for 40 min at 121 °C. To prevent precipitation and unwanted reactions in the medium, the glucose, trace salts (with KCl and betaine), phosphates and $MgSO_4$ were autoclaved separately and mixed after cooling. The KOH reservoir was also autoclaved, but it was filled with base afterwards.

The reactor was filled with 1.5 L of medium, and the CO_2 flow was established to maintain a positive pressure in the reactor. After stabilizing the pH and temperature, 20 ml of the inoculum was injected into the reactor through a rubber septum at the head of the reactor.

The dilution due to KOH dosing and removal of metabolites due to sampling were considered by calculating the batch data in grams produced and then dividing by the initial batch volume of 1.5 L. As large samples were required for DCW analysis, it was

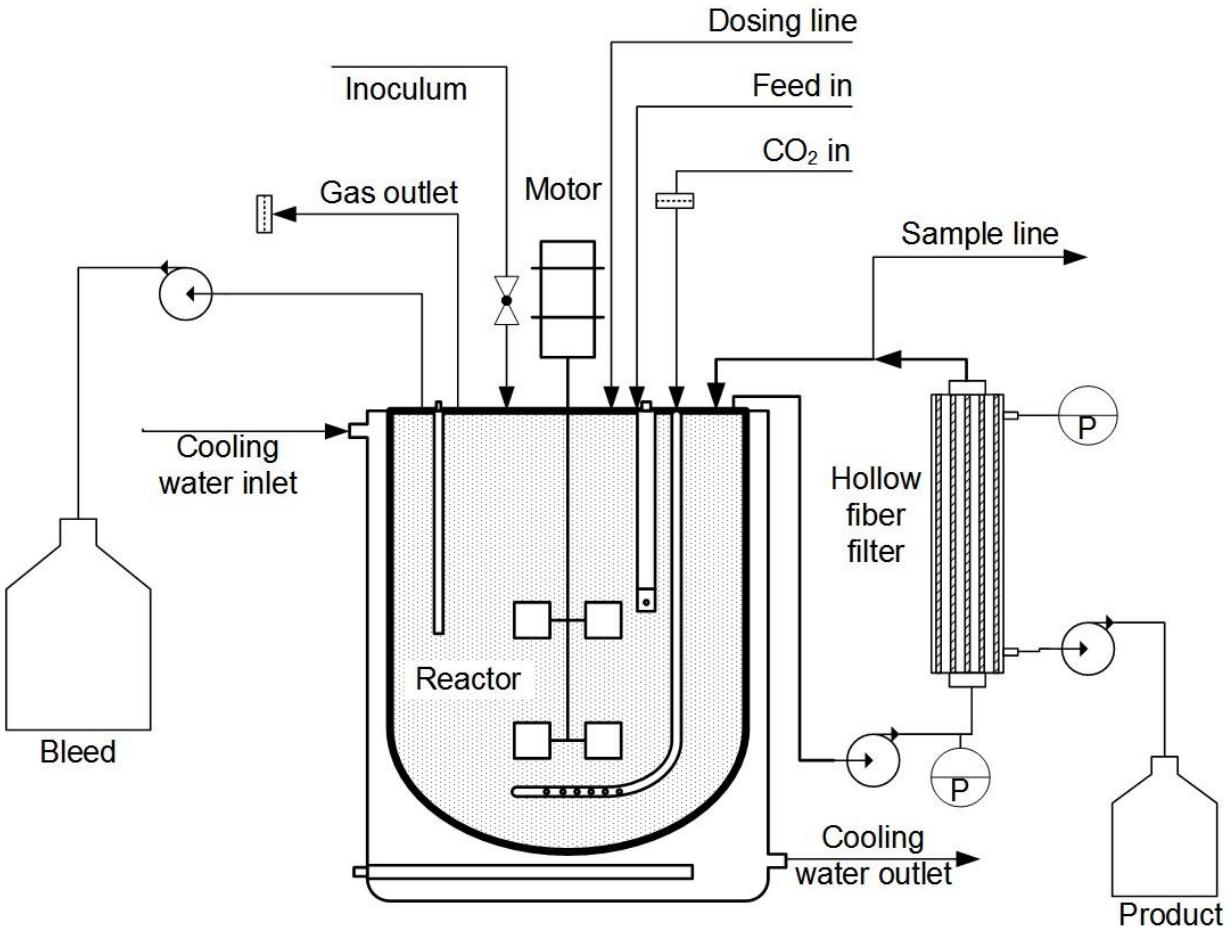

Figure 1: Simplified schematic of the reactor setup equipped for cell recycling

necessary to account for the substrate and metabolites removed. However, the batch volume remained very close to the initial volume throughout the fermentation, while the KOH dosing replaced the volume of the removed samples.

The volume at each sample point was calculated by adding the accumulated KOH dosing volume and subtracting the accumulated sample volume from the initial volume. The concentration of the produced succinate and acetate and the metabolized glucose was then calculated using Equation 1. For metabolites that decrease later in the batch (formate, pyruvate and DCW), the amount removed when sampling was not accounted for as the data on the metabolites are skewed, resulting in values far above the actual amounts in the reactor. Fortunately, these metabolites are present in considerably smaller quantities than the other metabolites, due to the drastic decrease in concentration later in the fermentation. Therefore, these metabolites were calculated using Equation 2:

$$C_i^* = \frac{1}{V_{t=0}}\left[C_i V + \sum_{s=1}^{i}\left(C_{i,sample} V_{sample}\right)\right] - C_{i,t=0} \quad (1)$$

$$C_i^* = \frac{\left(C_i V - C_{i,t=0} V_{t=0}\right)}{V_{t=0}} \quad (2)$$

2.5 Continuous fermentation with cell recycle

For continuous cell recycle fermentations, an autoclavable HFF was attached to the reactor. The HFF used consisted of a polysulphone membrane with a total membrane area of 1200 cm^2 and a nominal molecular weight cut-off pore size of 500,000 (UFP-500E-5A, GE Healthcare, Westborough, UK).The inlet and outlet of the HFF were connected to the reactor, using a peristaltic pump with a high flow rate to recirculate the medium at approximately 0.65 $L.min^{-1}$. Two autoclavable pressure gauges (EM

series, Anderson Instrument Co., Fultonville, NY, USA) were placed on the filter, one at the feed inlet and one on the permeate side of the filter, to calculate the transmembrane pressure (maintained at 0.3 bar) and to ensure that the inlet pressure did not exceed the maximum pressure rating. A pump was fitted on the permeate line to control the permeate flow rate and to supply a back pressure to the filter, thus reducing fouling.

The reactor was filled with 1.3 L of the medium for continuous fermentations, and it was first operated in batch fashion to accumulate sufficient biomass. The dilution rate and permeate flow rate were then set to the required value. The volume of the continuous fermentations was controlled by the bleed stream. The bleed rates varied between 10% and 13% of the feed stream, and no direct link was observed between bleed and dosing variation.

The steady state was determined by evaluating the KOH dosing flow 10 h before sampling. Variation within 10% of the average dosing flow rate was deemed sufficient to assume steady state. In order to assess the accuracy of the samples, a mass balance was applied to each sample. The glucose required to form the metabolic products and the removed cells (assuming an elemental composition of $CH_{1.8}O_{0.5}N_{0.2}$) could be calculated and compared with the experimental glucose consumed. The results presented as averaged values are given with standard deviation to show the variation in the values.

3 Results and Discussion

3.1 Comparative batch fermentations

The results from the three batch fermentation runs are given in Fig. 2. The initial glucose concentration varied between 90 and 102 $g.L^{-1}$. Runs 1 and 2 are repeat

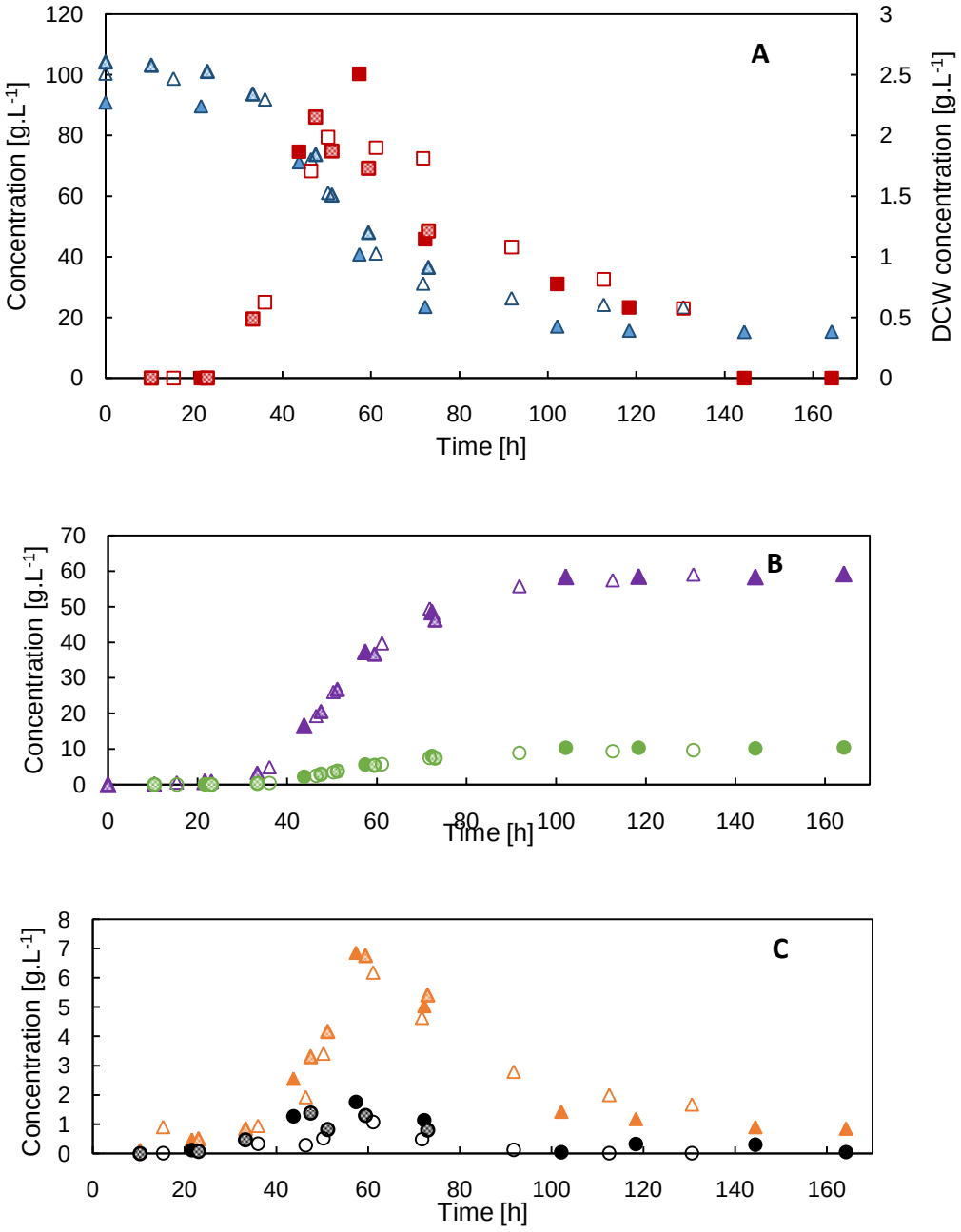

Figure 2: Metabolite concentration data of 3 separate batch fermentations indicating good repeatability despite an increase in the medium constituents of batch3. (Legend: A: Glucose, ▲ and DCW,■; B: succinate, ▲and acetate, ●; C: pyruvate, ▲ and formate, ●; The different batch fermentations are shown with a different marker fill: batch 1, ■; batch 2, ▩ andbatch 3, □).

runs, except for the premature termination of run 2 due to a CO_2 shortage. Run 3 was performed with 1.5 times the concentration of the standard AM1 medium (only the glucose concentration remained similar to the other runs) to test for media limitations. The good repeatability between the runs suggests that nutrient limitations had no effect on the production rates. The succinate production of runs 1 and 3 ceased towards the end of the fermentation, with sufficient glucose remaining in the fermenter (>20 $g.L^{-1}$) and the DCW of biomass approaching zero. Pyruvic and formate (see Fig. 2) had similar time profiles to that of the DCW, where these acids were consumed after the maximum DCW value had been achieved. The turning point of all three profiles (DCW, pyruvate and formate) occurred close to 25$g.L^{-1}$ succinate.

From the DCW turning point in Fig. 2, it is evident that cell death and subsequent lysis occur towards the end of the fermentation. The decreasing leg of the DCW profile indicates that the rate of cell death and lysis exceeds the rate of cell production after 60 h. Succinate production and pyruvate/formate consumption still occurred after 60 h, albeit at a much lower rate, suggesting that metabolic activity had not ceased completely. Unlike formate/pyruvate, no acetate consumption was observed in this latter period, suggesting that acetate is a terminal catabolite. Due to severe cell death, the DCW measurement contains a significant and unquantified amount of inactive cells. Accordingly, specific production rates (based on active mass of cells) cannot be determined or used for the fermentation analysis. The observed downward DCW trend is not unique to the observations of this study. Li et al.[20] used various organic acids in fermentations with modified *E. coli* NZN111and *E. coli* AFP111 strains. Succinate additions of 40 and 60 $g.L^{-1}$ resulted in an initial increase in broth OD, followed by a subsequent decrease for both strains.

The final averaged yield for the completed runs was 0.846 ± 0.0004 $g.g^{-1}$, with a final succinate titre of 59.1 ±0.06 $g.L^{-1}$. This is lesser than the batch yield of 0.96 $g.g^{-1}$ reported by Jantama et al.[12] who achieved final titres of up to 82.6 $g.L^{-1}$ in a fermentation with CO_2 supplied in the form of K_2CO_3, although they used the same fermentation medium and initial glucose concentrations as those used in the present study. At 100 h, 95% of all the succinate had been produced at an average productivity of 0.59 ±0.001 $g.L^{-1}h^{-1}$.

Numerous comparative fermentations have been reported for modified *E. coli* strains. All fermentations were batch, fed-batch or dual-phase fed-batch where aerobic conditions were initially used for cell accumulation. The review by Cheng et al.[21] contains a recent comprehensive list of these fermentations. Notably high yields were obtained by Vemuri[22] and by Sanchez in two studies[23,24] with reported mass-based yields of 0.96, 1.05 and 1.06 $g.g^{-1}$,respectively. The volumetric productivities of these high-yield fermentations were similar to those observed in this study, ranging from 0.4 to 0.6 $g.L^{-1}.h^{-1}$ with the maximum succinate titre (40 $g.L^{-1}$) lower than the batch result from this study.

3.2 Continuous fermentations

The runs were performed at dilution rates of 0.05, 0.10 and 0.15 h^{-1} in no specific order. A section of the results can be seen in Fig. 3. The amount of consumed glucose was used rather than the total glucose concentration, as the initial glucose concentration varied slightly during the continuous fermentations. Provided the steady-state criteria (see Section 2.5) were satisfied, at least four HPLC and DCW measurements were obtained within a steady state. All steady states at a given dilution rate (*D*) were maintained for at least 60 h. Two separate steady states were

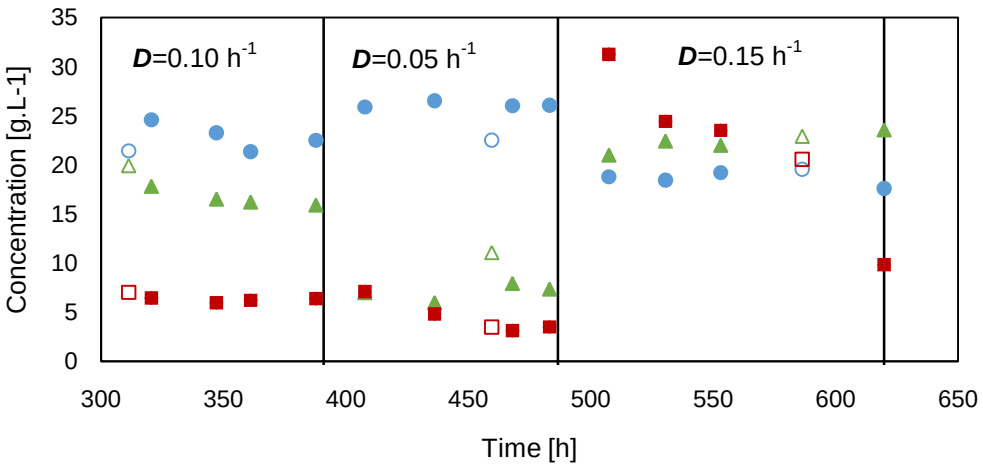

Figure 3: Time progression of cell recycle experiment showing a fraction of the total fermentation where 3 different dilution rates were covered. Note the DCW decrease for D=0.15 h^{-1}, despite metabolite stability. (Total glucose, ▲, succinate, ● and DCW, ■; open markers indicate non-steady state data where KOH dosing criteria werenot met).

performed for D = 0.1 h^{-1}. The averaged data with standard deviation bars are presented in Fig. 4, on which the metabolite concentrations, overall succinate yield and volumetric productivities are plotted. The standard deviation is based on 4, 7 and 4 samples at dilution rates of 0.05, 0.10 and 0.15 h^{-1} respectively.

The DCW readings tended to decrease during steady-state periods, whereas the metabolite concentrations and dosing flow rates remained constant (see Fig. 3). This suggests that the DCW measurement does not reflect the active amount of biomass and that the inactive fraction varied for different readings. The highest DCW was observed after the dilution rate was switched from 0.05 h^{-1} to 0.15 h^{-1} (Fig. 3), with an extremely high DCW reading of 31 $g.L^{-1}$ occurring directly after the switch. This was most probably caused by a rapid transient reduction in the succinate concentration, which enhanced the cellular growth rate. This corresponds to the behaviour under batch fermentation where the growth rate is closely linked to the product titre, that is, fast at low-titre conditions. It is interesting to note that the succinate productivity of the 507-h sample (Fig. 3) is similar to that of the 619-h sample, despite a threefold decrease in DCW (31–9.8 $g.L^{-1}$). This suggests that severe cell death occurs shortly after the growth spurt initiated at 483 h, whereas cell lyses occurred at a slower rate. DCW gradually declines until equilibrium is established between growth, death and lyses, as observed in the 0.05 h^{-1} responses in Fig. 3.

Figure 4 (A) only shows an increase in the succinate titre from 18 to 25 $g.L^{-1}$ as D decreases from 0.15 to 0.05 h^{-1}. This is a relatively small increase (39%) compared with the threefold decrease in throughput. From the batch results, evidently, net cell growth does not occur beyond a succinate titre of 25$g.L^{-1}$. However, succinate production does not cease beyond this terminal point, although it does decrease significantly. This production is most probably related to non-growth maintenance

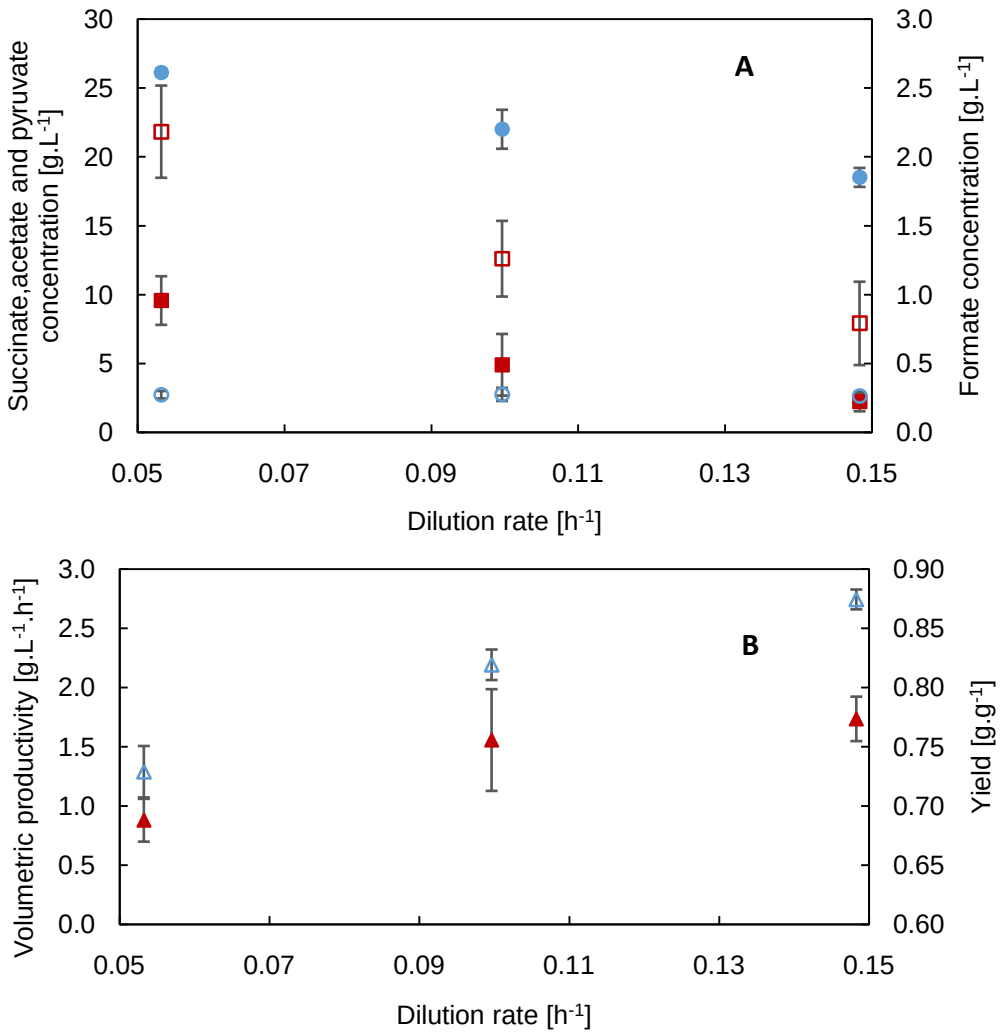

Figure 4: (A) Average metabolite concentration (succinate, ●, pyruvate, ■, acetate, o, and formate, □)and (B) yield, ▲, and volumetric productivity, △, for steady state measurements. Bars represent the standard deviation of all steady-state measurements.

processes of the remaining living cells in the system, although it could also be caused by growth occurring at a slower rate than cell lysis, resulting in a net decrease of DCW. The fact that the continuous succinate titre at very low *D* (0.05 h^{-1}) is similar to the critical batch titre (25g.L^{-1}) suggests that growth does not occur beyond this critical titre. This implies that continuous cultures are limited by the maximum achievable succinate titre close to 25 g.L^{-1}. This result will significantly affect the downstream processing costs, possibly outweighing the benefits of increased productivity.

From Fig. 4 (B), it is evident that volumetric productivity increases significantly at higher dilution rates. An average productivity of 2.74 ± 0.08 g.L^{-1}.h^{-1} was achieved at *D* = 0.15 h^{-1}, almost five times higher than the average batch productivity of 0.59 g.L^{-1}.h^{-1}. The productivity results can also be directly compared with the chemostat study by Van Heerden and Nicol[11] on *E. coli* KJ134 (which differs from KJ 122 only by the inactivation of phosphotransacetylase), who achieved a maximum productivity of 0.87 g.L^{-1}.h^{-1} at a *D* of 0.09 h^{-1}. This indicates that the high cell densities significantly enhance the volumetric productivity, especially when operating well below the growth termination succinate titre of 25 g.L^{-1}. The productivity trend in Fig. 4 (B) suggests that even higher productivities will be achieved at higher throughput (D), but at a lower succinate titre.

Reports of cell recycle succinate fermentation are rare in the open literature, especially with modified *E. coli* strains. Wang[25] used an ultrafiltration module to improve the performance of a fed-batch fermenter with modified *E. coli*. Although the differences in broth OD between the cell recycle and the system without any recycle were minimal, less by-product formation with cell recycle resulted in higher yields (0.7 g.g^{-1}) and succinate titre (70 g.L^{-1}). The volumetric productivity in this study remained low (0.4 g.L^{-1}.h^{-1}). Cell recycle with *A. succiniciproducens*[26] was the most successful, with a

productivity of 14.8 $g.L^{-1}.h^{-1}$ and a succinate yield of 0.83 $g.g^{-1}$. In addition to cell recycle, a fermenter with an electrodialysis unit, for removing organic acids in situ and thereby increasing the final product titre up to 80 $g.L^{-1}$, was presented. Biofilm systems can also be directly compared with cell recycle systems, where cells are retained within the fermenter by the immobilization properties of *A. succinogenes*.[27] Continuous biofilm runs have resulted in productivities exceeding 10 $g.L^{-1}.h^{-1}$ (Refs. [28, 29]), with reported yields as high as 0.9 $g.g^{-1}$.[13]

3.3 Metabolic flux and yield

The average mass balance closures for the respective dilution rates were 0.94 ± 0.03 (D = 0.05 h^{-1}), 0.95 ± 0.04 (D = 0.1 h^{-1}) and 1.05 ± 0.06 (D = 0.15 h^{-1}). These provide confidence in the accuracy of the measurements and suggest that all catabolites have been accounted for. Therefore, the tested continuous data set can be used in a proper metabolic flux analysis, in which the accountability of all catabolites is very important. In contrast to the continuous data set, the metabolic fluxes for the batch fermentations were not calculated, as the non-steady-state behaviour complicates the reconciliation of the measurements. Accordingly, only overall yields and general flux trends are discussed for the batch data, while proper flux quantification is performed for the steady state (cell recycle) data.

The metabolic flux model is based on the use of the oxidative TCA cycle to generate the reduction power required for homosuccinate fermentation.[11] It is also possible to use the glyoxylate shunt for the analysis. However, due to the direct similarity, only the oxidative TCA pathway was considered. A simplified version of the metabolic pathways of *E. coli* KJ 122 is presented in Fig. 5. Pathways of acetate and formate formation were included, despite their deletion, because significant amounts of

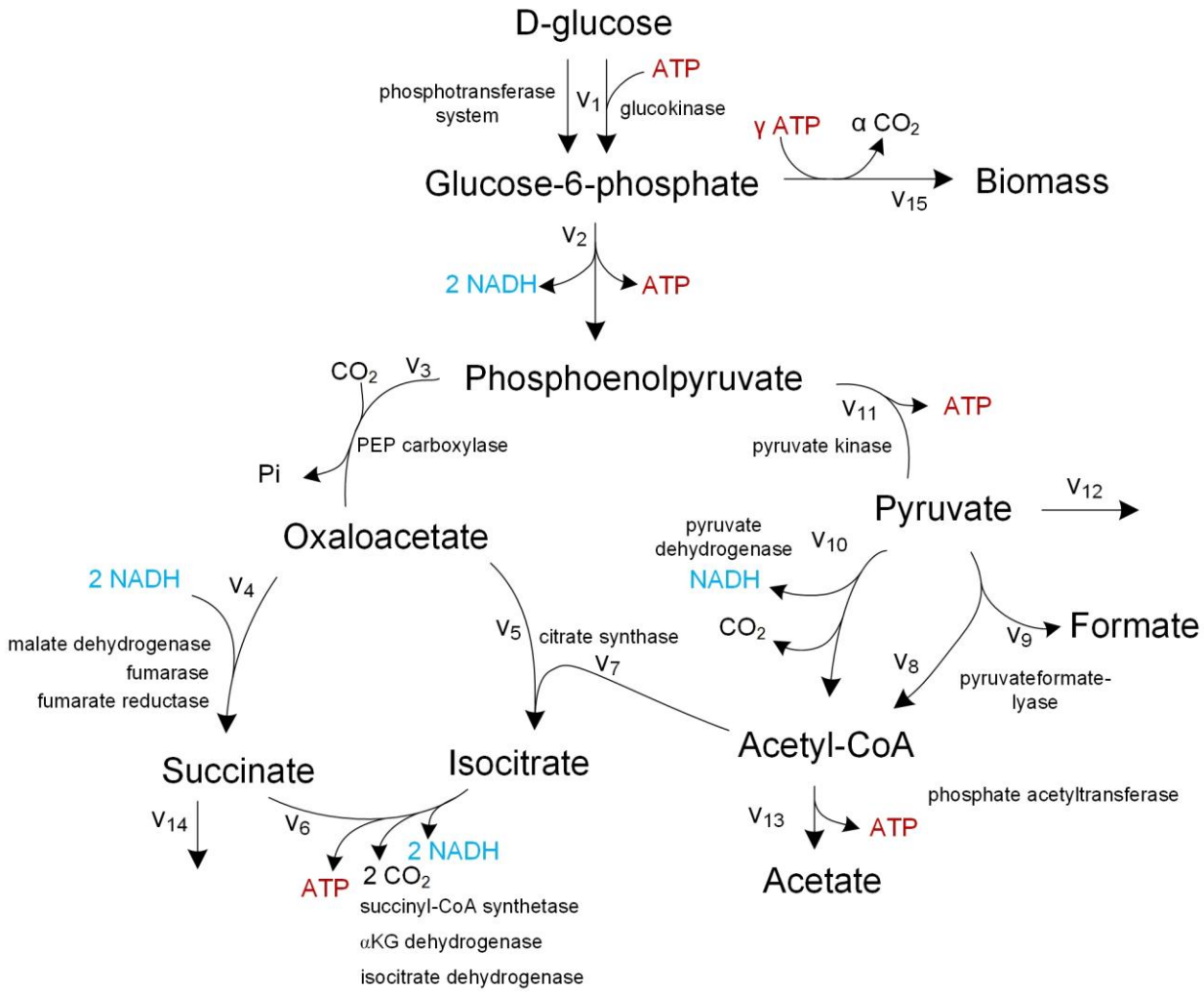

Figure 5: Simplified metabolic map employed for flux analysis. Fluxes used in Equations 3–6 are indicated on the pathways (Adapted from complete map given by Jantama et al., 2008)

formate and acetate were measured. Lactate and ethanol were not detected in any HLPC results and were therefore not included in the simplified metabolic pathway. The glucose uptake system is not specified in the flux model since no ATP balance was performed. No distinction could be made between pyruvate dehydrogenase and pyruvate formate lyase followed by formate dehydrogenase. Accordingly only pyruvate dehydrogenase was considered.The matrix-based description of the metabolic network was solved for each steady-state sample as shown by Nielsen et al.,[30] with closed carbon and nicotinamide adenine dinucleotide (NADH) balances within the presented pathway (Fig. 5). Given the catabolite measurements, the system was fully specified without considering the ATP balance; accordingly, the energy requirements were not considered in the analysis. (The complete equation matrix and flux values are available in the electronic annex).

The following dimensionless flux ratios represent the governing splits in the metabolic model:

$$PEP_{pyr} = v_{11}/v_2 \quad (3)$$

$$ACoA_{cit} = v_7/(v_7 + v_{13}\ ) \quad (4)$$

$$Pyr_{pd\,h} = v_{10}/(v_{10} + v_9 + v_8\ ) \quad (5)$$

$$Pyr_{out} = v_{12}/v_{11} \quad (6)$$

PEP_{pyr}(Equation 3) represents the fraction of the total carbon flux entering the oxidative TCA branch towards succinate and other by-products. $ACoA_{cit}$(Equation 4) quantifies the fraction of acetyl coenzyme A (acetyl-CoA) that enters the oxidative TCA cycle. Pyr_{pdh} (Equation 5) represents the fraction of pyruvate converted to acetyl-CoA through pyruvate dehydrogenase instead of through pyruvate formate lyase. Lastly,

Pyr_{out}(Equation 6) indicates the fraction of formed pyruvate that is excreted into the medium, probably due to a metabolic overflow from glycolysis.[12] For the perfect theoretical scenario,[11]Pyr_{out} should be zero, whereas Pyr_{pdh} and $ACoA_{cit}$ should be unity, whereby no formate, pyruvate or acetate is formed as catabolic products.

The results of the metabolic flux analysis are presented in Table 2. The average production rates for each dilution rate is given in Table 3, with the calculated glucose consumption. The significant amounts of acetate, formate and pyruvate excreted indicate the non-ideal and non-intended behaviour of the organism. The formation of formate suggests that the pyruvate formate lyase deletion is not effective under prolonged operation and that genetic regression to the original strain occurs. The relatively low and constant value of $ACoA_{cit}$ for all dilution rates indicates that minimal flux was directed towards the oxidative flux of the TCA and that acetate was predominantly formed, despite considerable efforts to terminate the flux.[12]Accordingly, the generation of NADH between isocitrate and succinate is not sufficient to eliminate by-product formation due to the overall redox requirements. $PEP_{pyr}$for homosuccinate fermentation will be 0.14 $cmol.cmol^{-1}$ (Ref. [11]), and the higher values obtained in the flux analysis reflect the significant amount of by-products formed.

The flux analysis results in Table 2 indicate that the flux distribution varies significantly with *D*. A significant decrease in pyruvate excretion is observed as D is increased. The Pyr_{out} ratio decreases with more than a factor of 2 when comparing $D=0.05h^{-1}$ to $D=0.15h^{-1}$.The decreased excretion is linked to less pyruvate formed from PEP (PEP_{pyr}) and more of the formed pyruvate converted via the dehydrogenase route (Pyr_{pdh}). A six fold increase in the pyruvate dehydrogenase flux is observed between 0.05 and $0.15h^{-1}$. It also likely that an activity increase in formate dehydrogenase is responsible for the observation since the flux analysis cannot distinguish between the

Table 2: Results from metabolic flux analysis with standard deviation

Dilution rate (h^{-1})	PEP_{pyr} ($cmol.cmol^{-1}$)	$ACoA_{cit}$ ($cmol.cmol^{-1}$)	Pyr_{pdh} ($cmol.cmol^{-1}$)	Pyr_{out} ($cmol.cmol^{-1}$)
0.05	0.43 ± 0.004	0.200 ± 0.01	0.19 ± 0.09	0.65 ± 0.04
0.10	0.38 ± 0.035	0.196 ± 0.02	0.50 ± 0.17	0.47 ± 0.15
0.15	0.34 ± 0.021	0.187 ± 0.01	0.68 ± 0.10	0.31 ± 0.07

Table 3: Average metabolic rates for each dilution rate, with the metabolized glucosecalculated from equation 1.

Dilution rate (h^{-1})	DCW ($g.L^{-1}.h^{-1}$)	Glucose consumed ($g.L^{-1}.h^{-1}$)	Calculated glucose ($g.L^{-1}.h^{-1}$)	Succinic acid ($g.L^{-1}.h^{-1}$)	Formic acid ($g.L^{-1}.h^{-1}$)	Acetic acid ($g.L^{-1}.h^{-1}$)	Pyruvic acid ($g.L^{-1}.h^{-1}$)
0.05	0.04 ± 0.002	2.1 ± 0.09	1.9 ± 0.09	1.4 ± 0.02	0.11 ± 0.02	0.15 ± 0.02	0.51 ± 0.12
0.10	0.06 ± 0.001	2.9 ± 0.15	2.8 ± 0.10	2.2 ± 0.14	0.13 ± 0.03	0.27 ± 0.05	0.49 ± 0.22
0.15	0.34 ± 0.038	3.6 ± 0.16	3.7 ± 0.24	2.7 ± 0.10	0.12 ± 0.04	0.39 ± 0.02	0.33 ± 0.10

two dehydrogenase routes. The end result is less formate is formed and more NADH is produced from oxidising pyruvate. It is exactly this additional reduction power that allows for more succinate production since the NADH demand in the reductive succinate branch controls the flux distribution at the PEP node. This is clear from the PEP_{pyr} ratio in Table 2 where more carbon is directed towards the reverse TCA branch at higher D. The end result is an increasing succinate yield at higher D. Lastly it is clear that the oxidative flux towards succinate remains minimal ($ACoA_{cit}$ ratio) and that most of the Acetyl-coA is converted to acetic acid. Improvement of this ratio will be crucial to further enhancing the succinate yield.

The best continuous yield of 0.77 $g.g^{-1}$ is less than the overall batch yield of 0.85 $g.g^{-1}$ and similar to the maximum chemostat yield of *E. coli* KJ134 of 0.77 $g.g^{-1}$.[11] The improvement in the batch yield can be mainly explained by the pyruvate and formate consumption in the batch run beyond a titre of 25 $g.L^{-1}$ (see Fig. 2). It is suspected that formate is metabolized by formate dehydrogenase under non-growth conditions (in the batch fermenter). This supplies the NADH that enables the accumulated pyruvate to flux towards succinate in the reductive section of the TCA pathway, thereby increasing the overall succinate yield.

4 Conclusion

The study investigated the feasibility of continuous HCDF with modified *E. coli* KJ122. It is apparent from the results that volumetric productivities can be significantly enhanced, but only below the critical succinate titre, close to 25 $g.L^{-1}$ of succinate. Evidence from batch and continuous runs suggests that growth above this critical titre is minimal or non-existent, while cell death is rapid and followed by lyses. This limits the achievable titre in continuous fermentations, while high volumetric productivities

are only possible at higher throughput where the succinate titre is lower than the critical value. This fermentation process can be successfully implemented with a separation process, wherein the product titre is not the main cost driver.

The steady-state data exhibited proper mass balance closure and allowed for an in-depth investigation into the internal flux distributions. It is evident that the oxidative flux to succinate is minimal, thus forcing the production of unwanted by-products. The overall succinate yield did increase with increasing dilution, mainly due to increased pyruvate dehydrogenase action. Unfortunately, the highest yields obtained are still on par with that of the native succinate producers where by-products such as acetate cannot be avoided.[13]Further, it is clear that the intended flux distribution did not fully succeed under conditions of high cell density.

Batch fermentation with *E. coli* KJ122 is still superior to continuous fermentation in terms of the final succinate titre and overall succinate yield. Its advantage includes the production of succinate due to the formate and pyruvate consumption during the non-growth period of the fermentation, despite the rapid cell death and lysis that occurs in this period. Nevertheless, the continuous high-cell-density productivity is far superior with values up to fivefold higher than the average batch productivities. A detailed cost analysis will be required to weigh the advantages against the disadvantages.

Acknowledgement

The financial contribution of the National Research Foundation (NRF) towards this research is hereby acknowledged.

References

[1] Bozell JJ, Petersen GR. Technology development for the production of biobased products from biorefinery carbohydrates – The US Department of Energy's 'Top 10' revisited. Green Chem 2010;12:539–54.

[2] Jansen MLA, van Gulik WM. Towards large scale fermentative production of succinic acid. CurrOpin Biotech 2014;30:190–97.

[3] Beauprez JJ, De Mey M, Soetaert WK. Microbial succinic acid production: Natural versus metabolic engineered producers. Process Biochem 2010;45:1103–14.

[4] Xu J, Guo BH. Poly(butylene succinate) and its copolymers: research, development and industrialization. Biotech 2010;5:1149–63

[5] Causey TB, Shanmugam KT, Yomano LP, Ingram, LO. Engineering *Escherichia coli* for efficient conversion of glucose to pyruvate. ProcNatlAcadSci USA 2004;101:2235–40.

[6] Thakker C, Martínez I, San KY, Bennett GN. Succinate production in *Escherichia coli*. Biotech J 2012;7:213–24.

[7] Zhang X, Jantama K, Shanmugam KT, Ingram LO. Reengineering *Escherichia coli* for succinate production in mineral salts medium. Appl Environ Microbiol 2009;75:7807–13.

[8] Vemuri GN, Eiteman MA, Altman E. Effects of growth mode and pyruvate carboxylase on succinic acid production by metabolically engineered strains of *Escherichia coli*, Appl Environ Microbiol 2002;68:1715–27

[9] Kwon Y, Lee S, Kim P. Influence of gluconeogenicphosphoenolpyruvatecarboxykinase (PCK) expression on succinic acid fermentation in *Escherichia coli* under high bicarbonate condition. J Microbiol Biotech 2006;16:1448–52.

[10] Blankschien MD, Clomburg JM, Gonzalez R. Metabolic engineering of *Escherichia coli* for the production of succinate from glycerol. MetabEng 2010;12:409–19.

[11] VanHeerden CD, Nicol W. Continuous and batch cultures of *Escherichia coli* KJ134 for succinic acid fermentation: metabolic flux distributions and production characteristics. Microb Cell Fact 2013;12:80-9.

[12] Jantama K, Zhang X, Moore JC, Shanmugam KT, Svoronos SA, Ingram LO. Eliminating side products and increasing succinate yields in engineered strains of *Escherichia coli* C., Biotech Bioeng 2008;101:881–93.

[13] Bradfield MFA, Nicol W. Continuous succinic acid production by *Actinobacillussuccinogenes* in a biofilm reactor: Steady-state metabolic flux variation. BiochemEng J 2014;85:1–7

[14] Chang H, Yoo I, Kim B. High density cell culture by membrane-based cell recycle. Biotech Adv 1994;12:467–87.

[15] Toda K. Theoretical and methodological studies of continuous microbial bioreactors. J Gen ApplMicrobiol 2003;49:219–33.

[16] Xu G, Chu J, Wang Y, Zhuang Y, Zhang S, Peng H. Development of a continuous cell-recycle fermentation system for production of lactic acid by *Lactobacillus paracasei*. Process Biochem 2006;41:2458–63.

[17] Cruz JM, Domínguez JM, Domínguez H, Parajó JC. Xylitol production from barley bran hydrolysates by continuous fermentation with *Debaryomyceshansenii.* Biotech Lett 2000;22:1895–98.

[18] Lee YL, Chang HN. High cell density culture of a recombinant *Escherichia coli* producing penicillin acylase in a membrane cell recycle fermenter. Biotech Bioeng 1990;36:330–37.

[19] Martinez A, Grabar TB, Shanmugam KT, Yomano LP, York SW, Ingram LO. Low salt medium for lactate and ethanol production by recombinant *Escherichia coli* B. Biotech Lett 2007;29:397–404.

[20] Li Q, Wang D, Wu Y, Yang M, Li W, Xing J, Su Z. Kinetic Evaluation of Products Inhibition to Succinic Acid Producers Escherichia coli NZN111, AFP111, BL21, and Actinobacillussuccinogenes 130ZT. J Microbiol 2010;48:290-296.

[21] Cheng KK, Wang GY, Zeng J, Zhang JA. Improved Succinate Production by Metabolic Engineering. Biomed Res Int 2013;2013:1-12.

[22] Vemuri GN, Eiteman MA, Altman E. Succinate production in dual-phase Escherichia coli fermentations depends on the time of transition from aerobic to anaerobic conditions. J IndMicrobiolBiot 2002;28:325–32.

[23] Sanchez AM, Bennett GN, San KY. Novel pathway engineering design of the anaerobic central metabolic pathway in Escherichia coli to increase succinate yield and productivity. MetabEng 2005;7:229-239.

[24] Sanchez AM, Bennett GN, San KY Batch culture characterization and metabolic flux analysis of succinate-producing Escherichia coli strains. MetabEng 2006;8:209-226.

[25] Wang C, Ming W, Yan D, Zhang C, Yang M, Liu Y, Zhang Y, Guo B, Wan Y, Xing J. Novel membrane-based biotechnological alternative process for succinic acid production and chemical synthesis of bio-based poly (butylene succinate) BioresourceTechnol 2014;156:6-13.

[26] Meynial-Salles I, Dorotyn S, Soucaille P. A New Process for the Continuous Production of Succinic Acid From Glucose at High Yield, Titer, and Productivity. BiotechnolBioeng 2008;99:129-135.

[27] Van Heerden CD, Nicol W. Continuous succinic acid fermentation by *Actinobacillussuccinogenes*. BiochemEng J 2013;73:5-11.

[28] Maharaj K, Bradfield MFA, Nicol W. Succinic acid-producing biofilms of *Actinobacillussuccinogenes*: reproducibility, stability and productivity. ApplMicrobiolBiot 2014;98:7379-7386.

[29] Brink HG, Nicol W. Succinic acid production with *Actinobacillussuccinogenes*: rate and yield analysis of chemostat and biofilm cultures. Microb Cell Fact 2014;13:111-123.

[30] Nielsen J, Villadsen J, Lidén, G. Bioreaction Engineering Principles. New York: Springer; 2011. p. 155

Annex: Metabolic flux analysis calculations.

Table A-1: The complete equation matrix used to solve the metabolic flux analysis, as per equation A-1. All the metabolite values should be given in C-mol.L^{-1}.

$$\bar{M} \times \bar{v} = \bar{c} \qquad \text{(A-1)}$$

$\bar{M}$																$\bar{c}$
1	-1	0	0	0	0	0	0	0	0	0	0	0	0	-1,1		0
0	1	-1	0	0	0	0	0	0	0	-1	0	0	0	0		0
0	0	4/3	-1	-1	0	0	0	0	0	0	0	0	0	0		0
0	0	0	1	0	1	0	0	0	0	0	0	0	-1	0		0
0	0	0	0	1	-3/2	1	0	0	0	0	0	0	0	0		0
0	0	0	0	0	0	-1	1	0	2/3	0	0	-1	0	0		0
0	0	0	0	0	0	0	-1/2	1	0	0	0	0	0	0		0
0	0	0	0	0	0	0	-1	-1	-1	1	-1	0	0	0	$\times \bar{v} =$	0
0	0	0	0	1	0	-2	0	0	0	0	0	0	0	0		0
0	1/3	0	-1/2	0	1/2	0	0	0	1/3	0	0	0	0	0		0
0	0	0	0	0	0	0	0	1	0	0	0	0	0	0		Formate
0	0	0	0	0	0	0	0	0	0	0	0	1	0	0		Acetate
0	0	0	0	0	0	0	0	0	0	0	1	0	0	0		Pyruvate
0	0	0	0	0	0	0	0	0	0	0	0	0	1	0		Succinate
0	0	0	0	0	0	0	0	0	0	0	0	0	0	1		DCW

Table A-2 : The complete solution matrix for each sample, with the steady state samples indicated by SS. All the values are given in C-mol.L^{-1}.

Sample	D	v1	v2	v3	v4	v5	v6	v7	v8	v9	v10	v11	v12	v13	v14	v15
1	0,05	0,83	0,83	0,51	0,65	0,03	0,03	0,014	0,06	0,03	0,10	0,32	0,13	0,12	0,68	0,00
2	0,05	0,66	0,63	0,39	0,49	0,03	0,03	0,014	0,05	0,03	0,07	0,24	0,10	0,08	0,52	0,03
3	0,10	0,77	0,74	0,48	0,60	0,04	0,04	0,020	0,05	0,02	0,10	0,26	0,09	0,09	0,64	0,03
4: SS	0,10	0,82	0,79	0,52	0,64	0,04	0,04	0,021	0,05	0,02	0,11	0,27	0,09	0,10	0,69	0,03
5	0,10	0,92	0,88	0,58	0,72	0,05	0,05	0,024	0,05	0,03	0,13	0,31	0,10	0,11	0,77	0,03
6: SS	0,10	0,86	0,82	0,53	0,67	0,04	0,04	0,021	0,05	0,03	0,11	0,29	0,10	0,10	0,71	0,03
7: SS	0,10	0,87	0,84	0,53	0,67	0,04	0,04	0,021	0,05	0,03	0,11	0,30	0,11	0,10	0,71	0,03
8: SS	0,10	0,93	0,92	0,56	0,70	0,04	0,04	0,021	0,06	0,03	0,08	0,36	0,19	0,09	0,75	0,01
9	0,15	0,85	0,83	0,54	0,68	0,05	0,05	0,025	0,05	0,02	0,11	0,28	0,10	0,10	0,73	0,02
10: SS	0,10	0,95	0,92	0,62	0,78	0,06	0,06	0,029	0,04	0,02	0,16	0,30	0,09	0,11	0,83	0,03
11: SS	0,10	1,01	0,98	0,59	0,74	0,04	0,04	0,022	0,05	0,03	0,07	0,39	0,24	0,07	0,79	0,02
12: SS	0,10	0,97	0,94	0,54	0,69	0,04	0,04	0,019	0,07	0,03	0,03	0,40	0,27	0,07	0,72	0,03
13: SS	0,10	1,00	0,97	0,57	0,72	0,04	0,04	0,022	0,07	0,04	0,05	0,40	0,24	0,08	0,76	0,03
14: SS	0,04	1,14	1,09	0,66	0,82	0,05	0,05	0,027	0,09	0,04	0,06	0,43	0,24	0,10	0,88	0,04
15: SS	0,05	1,22	1,20	0,67	0,85	0,05	0,05	0,023	0,11	0,06	0,01	0,52	0,35	0,09	0,90	0,02
16	0,05	1,09	1,07	0,57	0,73	0,04	0,04	0,018	0,11	0,06	-0,03	0,50	0,36	0,07	0,76	0,02
17: SS	0,06	1,21	1,19	0,66	0,85	0,04	0,04	0,018	0,08	0,04	0,03	0,53	0,38	0,08	0,88	0,02
18: SS	0,05	1,19	1,17	0,66	0,84	0,05	0,05	0,023	0,10	0,05	0,02	0,51	0,33	0,09	0,88	0,02
19: SS	0,14	0,93	0,74	0,48	0,60	0,04	0,04	0,021	0,05	0,02	0,09	0,26	0,10	0,09	0,64	0,18
20: SS	0,15	0,82	0,70	0,47	0,58	0,04	0,04	0,021	0,03	0,02	0,11	0,23	0,07	0,09	0,63	0,11
21: SS	0,15	0,86	0,75	0,49	0,61	0,04	0,04	0,020	0,04	0,02	0,11	0,26	0,09	0,10	0,65	0,10
22	0,14	0,80	0,71	0,50	0,62	0,04	0,04	0,022	0,01	0,00	0,15	0,21	0,04	0,09	0,66	0,08
23: SS	0,16	0,72	0,65	0,45	0,56	0,04	0,04	0,020	0,02	0,01	0,13	0,20	0,05	0,08	0,60	0,07